TMPRSS2, required for SARS-CoV-2 entry, is downregulated in lung cells by enzalutamide, a prostate cancer therapeutic

Damien A. Leach
Imperial College London
Ana-Maria Isac
University of Essex
Charlotte L. Bevan (charlotte.bevan@imperial.ac.uk)
Imperial College London
Greg N. Brooke (gbrooke@essex.ac.uk)
University of Essex

Research Article

Keywords: COVID-19, SARS-CoV-2, androgen receptor, antiandrogens, lung, TMPRSS2, ACE2

Posted Date: June 10th, 2020

DOI: https://doi.org/10.21203/rs.3.rs-34503/v1

Version of Record: A version of this preprint was published at Nature Communications on June 10th, 2020. See the published version at https://doi.org/10.1038/s41467-021-24342-y.

TMPRSS2, required for SARS-CoV-2 entry, is downregulated in lung cells by enzalutamide, a prostate cancer therapeutic

D. A. Leach[1], A.M. Isac[2], C. L. Bevan[1*], G. N. Brooke[2*]
[1] Department of Surgery and Cancer, Imperial College London, London W12 0NN, UK
[2]School of Life Sciences, University of Essex, Wivenhoe Park, Colchester, ESSEX, CO4 3SQ
*Joint corresponding/senior authors; these authors contributed equally

ABSTRACT
The COVID-19 pandemic, caused by the SARS-CoV-2 coronavirus, attacks various organs but most destructively the lung. It has been shown that SARS-CoV-2 entry into lung cells requires two host cell surface proteins: ACE2 and TMPRSS2. Downregulation of one or both of these is thus a potential therapeutic approach for COVID-19. TMPRSS2 is a known target of the androgen receptor, a ligand-activated transcription factor; activation of the androgen receptor increases TMPRSS2 levels in various tissues, most notably the prostate. We show here that treatment with the antiandrogen enzalutamide – a well-tolerated drug widely used in advanced prostate cancer – reduces TMPRSS2 levels in human lung cells. Further, enzalutamide treatment of mice dramatically decreased Tmprss2 levels in the lung. In support of this new experimental data, analysis of existing datasets shows striking co-expression of AR and TMPRSS2, including in specific lung cell types that are targeted by SARS-CoV-2. Together, the data presented provides strong evidence to support clinical trials to assess the efficacy of antiandrogens as a treatment option for COVID-19.

KEYWORDS
COVID-19, SARS-CoV-2, androgen receptor, antiandrogens, lung, TMPRSS2, ACE2

INTRODUCTION
Severe acute respiratory syndrome coronavirus 2 (SARS-CoV-2), the cause of the COVID-19 pandemic, is a positive-sense single-stranded RNA coronavirus highly related to SARS-CoV, which caused the 2002 SARS pandemic [1, 2]. Like SARS, COVID-19 primarily affects the respiratory system (although other organs can also be affected): symptoms are mild in some, but in others the infection can result in pneumonia, Acute Respiratory Distress Syndrome (ARDS) and death [3]. Risk factors associated with poor prognosis include age, diabetes and cardiovascular disease [4]. It has also been shown that gender is a prognostic factor, with approximately 60-70% of deaths being in men [5, 6], suggesting that steroid hormones may be a contributing factor to the severity of the disease. In further support of this, recent studies have shown that men with male pattern hair loss (caused by elevated androgen signalling [7]), are at higher risk of suffering more severe COVID-19 symptoms [8, 9].

Coronoviruses have structural (Spike, Nucleocaspid, Matrix and Envelope) and non-structural (e.g. the proteases nsp3 and nsp5) proteins [10]. Viral entry is reliant on two host proteins present on the surface of epithelial cells in the target organ: Transmembrane Serine Protease 2 (TMPRSS2) and Angiotensin-Converting Enzyme 2 (ACE2) [11]. TMPRSS2 primes the viral Spike (or S) protein by cleaving it at two sites; this facilitates fusion of the viral and host membranes [12-14]. Cellular entry is subsequently facilitated by ACE2, a terminal carboxypeptidase and type I transmembrane glycoprotein [15]. Thus, viral entry may be prevented or slowed by inhibition of ACE2 and/or TMPRSS2. TMPRSS2 is an attractive target

as knockout of this protein causes no overt detrimental phenotype [16], whereas ACE2 downregulation is associated with increased severity of SARS-induced lung injury [17]. Further, TMPRSS2 expression levels have been shown to be associated with disease severity in mouse models of coronavirus infection [18], and its inhibition was recently shown to inhibit SARS-2-S-driven entry in lung cells [11].

Multiple studies have shown that TMPRSS2 is an androgen receptor (AR) target gene in prostate cancer cells (e.g. [19-21]). The AR is a nuclear receptor and member of the steroid receptor family. It is a transcription factor activated by ligand binding, upon which it translocates from the cytoplasm to the nucleus where it binds to regulatory regions of target genes as a homodimer. Following the recruitment of accessory proteins and the basal transcriptional machinery, the active receptor promotes gene transcription [22]. In the case of prostate cancer, active AR promotes tumour growth and so treatment options for prostate cancer often target this signalling axis, through the use of androgen deprivation and hormonal therapies such as antiandrogens [23, 24]. Antiandrogens (e.g. Bicalutamide and Enzalutamide) interact with the AR in the ligand binding pocket and hold the receptor in an inactive conformation, unable to form an active transcriptional complex, and thus inhibit its activity.

Importantly, previous studies have demonstrated that the AR is expressed in the lung [25] and studies using mice have confirmed that AR is functional in this organ [26, 27]. In corroboration, *in vitro* studies have shown that multiple lung lines express functional AR [26, 28-30]. It is therefore possible that inhibition of androgen signalling, in response to antiandrogens, will reduce TMPRSS2 expression in the lung and reduce viral entry. For this reason, antiandrogens have been proposed as a treatment option for COVID-19 [31-33]. Here we review and reanalyse available data to investigate AR and TMPRSS2 in the lung, and provide additional pre-clinical data to support the use of antiandrogens for the treatment of COVID-19.

METHODS

Ligands

Mibolerone was purchased from Perkin Elmer (MA, USA) and dissolved in ethanol. Enzalutamide was from Sigma Aldrich (MO, USA) and was resuspended in DMSO.

Cell Culture

A549 and LNCaP were purchased from the ATCC (VA, USA) and were cultured in Dulbecco's Modified Eagle's Medium (DMEM) and Roswell Park Memorial Institute (RPMI) medium 1640 (Invitrogen, Strathclyde, UK) respectively, as previously described [34].

Immunoblotting

Cells were lysed in RIPA buffer (150 mM NaCl, 1 % IGEPAL CA-630, 0.5 % sodium deoxycholate, 0.1 % SDS, 25 mM Tris pH 7.4) containing freshly added protease inhibitors (Halt Protease Cocktail, ThermoFisher, MA, USA). Samples were incubated on ice for 10 min, sonicated 4 cycles of 30 sec on/off (Biorupter, Diagenode, NJ, USA) and centrifuged (13,000 rpm, 10 min, 4 °C). The DC protein assay (BioRad) was used to quantify protein concentrations. 30 μg of protein was separated using SDS-PAGE and immunoblotting performed, as previously described [35]. Rabbit anti-AR (ab74272, Abcam, Cambridge, UK) and mouse α-tubulin (B-5-1-2, Sigma Aldrich) primary antibodies were used at a concentration of 1:1000 and 1:10,000 respectively. Secondary HRP-conjugated antibodies (Sigma Aldrich) were used at 1:2000.

Proteins were visualised using Immobilon Forte HRP substrate (Merck Millipore, MA, USA) and a Fusion FX Chemi Imager (Vilber Lourmat, Collégien, France).

Quantitative PCR analysis of gene expression in cell lines

Cells were seeded in 12 well plates and incubated + 10 nM mibolerone ± 10 μM enzalutamide for 48 or 72 hrs. RNA was extracted using Trizol (Thermo Fisher), following the manufacturer's instructions. 250 ng of RNA was reverse transcribed using a LunaScript RT SuperMix Kit (NEB, MA, USA). Alterations in gene expression were quantified using the Luna Universal qPCR Master Mix (NEB) and a Roche 96 qPCR machine (Basel, Switzerland). *TMPRSS2* data were normalised to *L19* data and the $2^{(-\text{delta delta CT})}$ method was used to calculate gene expression changes. Human qPCR primers: (5'-3') TMPRSS2 forward – CTGCTGGATTTCCGGGTG, TMPRSS2 reverse – TTCTGAGGTCTTCCCTTTCT; L19 forward – GCGGAAGGGTACAGCCAAT, L19 reverse GCAGCCGGCGCAAA.

Mouse studies

Pten$^{loxp/loxp}$;*Pb-Cre4* mice (The Jackson Laboratory), which have prostate-specific PTEN deletion [36], were treated with 50 mg/kg Enzalutamide (in 5% DMSO +1% CMC +0.1% P80 oral gavage) or vehicle control every day for three days. All work was carried out in accordance with the provisions of the Animals (Scientific Procedures) Act 1986 of the United Kingdom and under an appropriate Home Office license. Organs were snap frozen until RNA was extracted using a Monarch RNA extraction kit (NEB) following disruption of frozen tissue utilizing mechanical disruption and enzymatic digestion with Proteinase K. 2 μg of RNA was reversed transcribed using Precision Nanoscript2 Rt Kit (Primer Design, Southampton, UK). Changes in gene expression were measured using SYBR Green Fast Master Mix (Life Technologies, CA, USA) and QuantStudio 7 Flex Real-Time PCR System (Applied Biosystems, CA, USA). Gene expression data were normalised to *L19, Gapdh,* and *Actb* data and the $2^{(-\text{delta delta CT})}$ method used to calculate changes in expression. Mouse qPCR primers (5'-3'): Tmprss2 forward – GAGAACCGTTGTGTTCGTCTC, Tmprss2 reverse – GCTCTGGTCTGGTATCCCTTG; Ace2 forward – TGATGAATCAGGGCTGGGATG, Ace reverse – ATTCTGAAGTCTCCGTGTCCC, Ar forward – TGGGACCTTGGATGGAGAAC, Ar reverse – CTCCGTAGTGACAGCCAGAAL19, Gapdh forward –GCAAAGTGGAGATTGTTGCCAT, Gapdh forward – CCTTGACTGTGCCGTTGAATTT, L19 forward – GAAATCGCCAATGCCAAC, L19 reverse – TCTTAGACCTGCGAGCCTCA, β-actin forward – CCTCTATGCCAACACAGTGC, β -actin reverse – CCTGCTTGCTGATCCACATC.

Analysis of TMPRSS2 expression in tissue and cell line datasets

RNA-sequencing dataset v8 was downloaded from the Genotype-Tissue Expression (GTEx) Project Online Portal [37]. Gene expression was normalized (inverse normal transformation) across samples, and medians for AR and TMPRSS2 expression across each tissue was calculated. Data from RNA sequencing of isolated single nuclei, performed on surgical specimens of healthy, non-affected lung tissue from twelve lung adenocarcinoma (LADC) patients, was analysed for AR, TMPRSS2, and ACE2 expression using Eils Lab UCSC Cell browser (https://eils-lung.cells.ucsc.edu) [38]. Sequencing data from MCF7 cell lines treated with 10 nM DHT or equivalent control (GSE99626), T47D cells treated with 10 nM DHT (GSE62243) [39], and data from lungs of castrated or intact mice (GSE31341) [40] were log2 transformed. Significance was determined by ANOVA.

Identification of potential AREs

The AR binding motif, MA0007.2 was obtained from the JASPAR online curated motif database [41]. Segments of DNA around the TMPRSS2 gene were scanned for potential matches for presence of the MA0007.2 AR motif using FIMO [42]. Of the 40 possible MA0007.2 matches in regulatory region 1 ($P<0.0001$) and 34 possible matches in regulatory region 2 ($P<0.0001$), only response elements that correlated with binding peaks were selected.

Analysis of ChIP-sequencing data

ChIP sequencing data (receptors in the presence of their cognate ligands) were analysed using Cistrome Analysis Pipeline and visualised with WashU Epigenome Browser (v51.0.5). Datasets used: LNCaP - AR (GSE94682) [43], H3K27ac (GSE73783) [44], FOXA1 (GSE94682) [43] and NR3C1/GR (GSE39880) [45]; A549 - H3K27ac (GSE29611) [46], FOXA1 (GSE32465) [47], JUN (GSE92812) [46] and NR3C1/GR (GSE91313) [46]; MC7 - AR (GSE104399) [48], H3K27ac (GSE94804) [49], FOXA1 (GSE112969) [50], JUN (GSE102410) [51] and NR3C1/GR (GSE39879) [45].

RESULTS AND DISCUSSION

TMPRSS2 is an androgen and antiandrogen-regulated gene

ACE2 and TMPRSS2 are crucial for SARS-CoV-2 entry into cells [11], and hence these receptors represent potential therapeutic targets for COVID-19. TMPRSS2 has been shown to be an AR target gene in prostate cancer (e.g. [19-21]) and we therefore hypothesised that the expression of the gene could be down-regulated in response to antiandrogens. To confirm this, the AR-positive prostate cancer cell line LNCaP was seeded in hormone-depleted media for 72 hrs and treated with the synthetic androgen mibolerone (MIB, 1 nM) and/or the antiandrogen enzalutamide (ENZA, 10 μM) for 24 hrs. Alterations in gene expression were quantified using qPCR. As expected, the addition of androgen significantly increased *TMPRSS2* expression (approximately 35-fold, Figure 1A). Importantly, enzalutamide successfully blocked this androgen-induced up-regulation, resulting in an almost complete inhibition of *TMPRSS2* expression. To determine whether AR regulation of TMPRSS2 also occurs in other cell types, gene expression was investigated in two breast cancer cell lines, MCF-7 (GSE99626) and T47D (GSE62243) [39]. In agreement with the LNCaP results, TMPRSS2 was also found to be upregulated in response to androgen in the breast lines, albeit weakly (Figure 1B and C).

TMPRSS2 and the AR are co-expressed in the lung

Androgen signalling is known to be important in multiple tissues/organs. To better characterise this signalling, we previously created the AR-LUC transgenic mouse in which luciferase expression is under the control of an androgen responsive promoter, allowing for visualisation of both *in vivo* and *ex vivo* AR activity. AR signalling was found to be active in a number of tissues/organs, including the prostate, seminal vesicles, uterus and ovaries – and importantly, AR signalling was also found to be active in the lungs of male and female mice, although activity was weaker than in the reproductive organs [27]. Other studies have also demonstrated that AR signalling is active in the lung. For example, Mikonnnen *et al.* found the AR to be predominantly expressed in type II pneumocytes and the bronchial epithelium and microarray analysis of the murine lung, and demonstrated that genes involved in oxygen

transport (among other pathways) are up-regulated in murine lung in response to androgen [26].

To investigate AR and TMPRSS2 expression in different human tissues, we interrogated the Genotype Tissue Expression (GTEx) dataset [52]. We found that AR and TMPRSS2 are co-expressed in a number of tissues, and generally, TMPRSS2 is only expressed in tissues that also show detectable levels of the AR, with the exception of the pancreas (Figure 2A). Importantly, AR and TMPRSS2 were found to be co-expressed in the lung (highlighted red, also highlighted are prostate, breast (both co-expressing) and pancreas). Analysis of single cell sequencing data from lung tissue [38], demonstrated that the AR is expressed in most cell types, with highest expression in club (bronchiolar exocrine cells), alveolar type 2 (AT2), fibroblast and endothelial cells. TMPRSS2 was found to have a fairly uniform expression across cell types, but was most highly expressed in the AT1 and AT2 luminal cells (Figure 2B,C). Significantly, these are the cell types targeted by SARS-CoV-2 [53]. AT1 and AT2 cells also demonstrated highest ACE2 expression, and measurable AR expression.

TMPRSS2 expression in the lung is higher in men

In adults, men have on average 7-8 times higher levels of circulating testosterone compared to women [54]. It was therefore hypothesised that TMPRSS2 expression would be higher in male lungs compared to females. Analysis of the GTEx dataset confirmed this, with TMPRSS2 expression significantly higher in the male lung (Figure 3). Interestingly, there was no significant difference in AR expression levels between men and women, suggesting the higher levels of TMPRSS2 expression are a result of increased AR activity due to circulating androgen levels, rather than higher AR levels. This would support the theory that the observed worse prognosis in men following SARS-CoV-2 infection (60-70% of COVID-19-related deaths are in men [5, 6]) is at least in part due to elevated expression of TMPRSS2 as a consequence of higher levels of androgen. In light of the recent studies linking male pattern hair loss with more severe COVID-19 symptoms [8, 9], it would be of interest to compare TMPRSS2 expression levels in men with and without this androgen-associated form of hair loss.

TMPRSS2 expression is reduced by enzalutamide in A549 cells

As discussed above, the AR is expressed in human and murine lung, and has been shown to be active. To investigate AR regulation of TMPRSS2 in the lung, we used the A549 human type II pneumocyte cell line; a cell type targeted by SARS-CoV-2 [53]. Immunoblotting confirmed AR expression: in agreement with the GTEx data, the AR is expressed in the lung cell line and levels are approximately 10-fold lower than in the prostate LNCaP line (Figure 4A).

TMPRSS2 expression has been previously shown to be androgen-regulated in the A549 cell line [18]. To replicate these findings, we seeded A549 cells in hormone-depleted media (containing serum that has been charcoal-stripped to remove any traces of hormones) for 3 days and treated with the synthetic androgen MIB. However, under these conditions *TMPRSS2* was undetectable by qPCR (data not shown). The experiment was therefore repeated for A549, and LNCaP, in media supplemented with 10% full serum, with/without enzalutamide. Fetal calf serum has been shown to contain castrate levels of testosterone, which LNCaP cells metabolise to produce physiologically relevant intracellular levels of dihydrotestosterone, sufficient to promote their growth [55]. Since this might not be the case in A549 cells, a final concentration of 10nM MIB was also added to both cell lines throughout the experiment. In these conditions, TMPRSS2 was expressed at detectable levels and,

importantly, enzalutamide potently down-regulated *TMPRSS2* expression in both LNCaP and A549 after 48 and (more so) 72 hours (Figure 4B). This therefore confirms that antiandrogens could be used to down-regulate TMPRSS2 expression in lung cells.

TMPRSS2 expression is reduced by enzalutamide in mouse lung

To investigate the effects of enzalutamide, on TMPRSS2 expression *in vivo*, mice were treated for three days with enzalutamide or vehicle control. Following sacrifice, lung tissue was collected and qPCR performed to quantify alterations in gene expression. While there was no significant change in *Ar* or *Ace2* expression, *Tmprss2* expression was significantly decreased after enzalutamide treatment ($P<0.05$, Figure 5A). To validate these findings, expression data from intact mice and mice that had been castrated (removal of testicular production of androgen) were interrogated (GSE31341) [40]. In agreement with our cell line data, castration significantly reduced *Tmprss2* expression in the mouse lung (Figure 5B). In the same mice, castration was also associated with an increase in *Ar* expression ($P<0.01$), expected as *Ar* gene transcription is downregulated in response to androgen [56].

TMPRSS2 expression in lung is potentially directly regulated by nuclear receptor proteins and coregulators.

Although ChIP-Seq data for genomic AR binding in lung tissue or cells is not available, we were able to assess the cistrome of FOXA1 and JUN, known pioneer coregulatory factors for the AR [57] and other nuclear receptors. Binding of the glucocorticoid receptor (GR) was also investigated as this can bind to many of the same response elements as the AR [58], also acetylated histone 27 (H3K27ac) as an indicator of active regulatory regions, all in A549 lung cells (Figure 6A). Binding profiles for prostate (LNCaP) and breast (MCF-7) cell lines were included for comparison. In LNCaP cells the AR binding pattern correlates with previous findings [20], and confirms that AR and GR bind in the same regions, corresponding also to binding of the pioneer factor FOXA1, and these sites largely correlate with the marker of transcriptionally active regions, H3K27ac. Detailed analysis of these potential response elements by the Claessens lab demonstrated that an androgen response element in the enhancer region (approximately -13 kb from the transcription start site) is crucial for optimal androgen regulation of TMPRSS2 in prostate cells [20].

The binding patterns of GR, pioneer factors and H3K27ac in lung cells, however, differ to what is seen in LNCaP cells (compare regulatory region 1 and 2). To assess if androgen response elements are present in regulatory region 2, the AR binding motif (MA0007.2, Figure 6B) from the JASPAR database, was used to detect AR target sites using methods previously described [31]. This analysis identified potential androgen response elements throughout the 5' region of the TMPRSS2 gene (Figure 6A and 6C). Importantly, several of the potential androgen response elements were found to correlate with the GR, FOXA1, JUN, and H3K27ac peaks seen in the A549 regulatory region 2. Together, this suggests that AR (and associated factors) may directly regulate TMPRSS2 via different regulatory regions in lung and prostate.

The DNA-binding of AR, GR, FOXA1, JUN, and H3K27ac around the TMPRSS2 gene in breast cancer cells (MCF-7) appears to be less pronounced than in prostate and lung, and the binding pattern has elements of the binding patterns in both prostate and lung cells. Importantly, AR binding in MCF-7 cells correlates with the H3K27ac, FOXA1, JUN and GR peaks located distally in the A549 regulatory region 2. This therefore provides further evidence that this region contains a functional androgen response element(s). Intriguingly, this region also correlates with a peak for oestrogen receptor-α (ESR1) binding in MCF-7. This supports the

possibility of TMPRSS2 regulation by other members of the nuclear receptor superfamily, and hence further potential for pharmacological manipulation by their ligands – in this case oestrogens/antioestrogens as well as, via the GR, glucocorticoids, DHT/antiandrogens via the AR.

CONCLUSIONS

The data presented here confirm a role for AR in regulation of TMPRSS2 in the lung, which may at least in part explain why men with COVID-19 have a worse prognosis compared to women. Data from prostate and breast tissue also support regulation in other organs, which may also be targeted by SARS-CoV-2. Importantly, our findings support the hypothesis that therapies to target AR signalling could be used to transcriptionally inhibit lung TMPRSS2 expression. Further, potential regulation of TMPRSS2 by other, related receptors (revealed by cistromic analysis) opens up the possibility of additional potential opportunities for pharmacological inhibition of TMPRSS2 expression. Down-regulation of TMPRSS2 will result in attenuated spike protein priming, reducing SARS-CoV-2 interaction with ACE2, blocking viral entry (summarised in Figure 7). Antiandrogens are used routinely in, or have been trialled for, the treatment of multiple diseases, including prostate cancer, breast cancer, polycystic ovarian syndrome and alopecia [59]. They have been shown to be well tolerated in men and women [59-61] and therefore antiandrogens should be considered as a potential therapeutic strategy for COVID-19.

ACKOWLEDGMENTS

D. Leach was funded by the Imperial College London COVID Fund and Prostate Cancer Foundation and A.M. Isac was funded by the University of Essex PhD Scholarship scheme. We would like to thank Piers Aitman for discussion and image design/processing and Gilberto Serrano de Almeida for assistance with *in vivo* experiments. We would also like to thank the Brooke and Bevan labs, Antonio Marco, Ralf Zwacka, Andrea Mohr and Efstathios Giotis for discussion of the project and Lynwen James for assistance with cell culture. Finally, we are extremely grateful to the technical staff at the University of Essex for providing laboratory support during the lockdown. The GTEx project is supported by multiple funding bodies NIH, NCI, NHGRI, NHLBI, NIDA, NIMH, and NINDS.

REFERENCES

1. Zhou, P., et al., *A pneumonia outbreak associated with a new coronavirus of probable bat origin.* Nature, 2020. **579**(7798): p. 270-273.
2. Ksiazek, T.G., et al., *A novel coronavirus associated with severe acute respiratory syndrome.* N Engl J Med, 2003. **348**(20): p. 1953-66.
3. Yuki, K., M. Fujiogi, and S. Koutsogiannaki, *COVID-19 pathophysiology: A review.* Clin Immunol, 2020. **215**: p. 108427.
4. Zhang, J., et al., *Risk factors for disease severity, unimprovement, and mortality in COVID-19 patients in Wuhan, China.* Clin Microbiol Infect, 2020. **26**(6): p. 767-772.
5. Chen, N., et al., *Epidemiological and clinical characteristics of 99 cases of 2019 novel coronavirus pneumonia in Wuhan, China: a descriptive study.* Lancet, 2020. **395**(10223): p. 507-513.
6. Jin, J.M., et al., *Gender Differences in Patients With COVID-19: Focus on Severity and Mortality.* Front Public Health, 2020. **8**: p. 152.

7. Ustuner, E.T., *Cause of androgenic alopecia: crux of the matter.* Plast Reconstr Surg Glob Open, 2013. **1**(7): p. e64.
8. Wambier, C.G., et al., *Androgenetic Alopecia Present in the Majority of Hospitalized COVID-19 Patients - the "Gabrin sign".* J Am Acad Dermatol, 2020.
9. Goren, A., et al., *A preliminary observation: Male pattern hair loss among hospitalized COVID-19 patients in Spain - A potential clue to the role of androgens in COVID-19 severity.* J Cosmet Dermatol, 2020.
10. Ibrahim, I.M., et al., *COVID-19 spike-host cell receptor GRP78 binding site prediction.* J Infect, 2020. **80**(5): p. 554-562.
11. Hoffmann, M., et al., *SARS-CoV-2 Cell Entry Depends on ACE2 and TMPRSS2 and Is Blocked by a Clinically Proven Protease Inhibitor.* Cell, 2020. **181**(2): p. 271-280.
12. Glowacka, I., et al., *Evidence that TMPRSS2 activates the severe acute respiratory syndrome coronavirus spike protein for membrane fusion and reduces viral control by the humoral immune response.* J Virol, 2011. **85**(9): p. 4122-34.
13. Matsuyama, S., et al., *Efficient activation of the severe acute respiratory syndrome coronavirus spike protein by the transmembrane protease TMPRSS2.* J Virol, 2010. **84**(24): p. 12658-64.
14. Shulla, A., et al., *A transmembrane serine protease is linked to the severe acute respiratory syndrome coronavirus receptor and activates virus entry.* J Virol, 2011. **85**(2): p. 873-82.
15. Jia, H., *Pulmonary Angiotensin-Converting Enzyme 2 (ACE2) and Inflammatory Lung Disease.* Shock, 2016. **46**(3): p. 239-48.
16. Kim, T.S., et al., *Phenotypic analysis of mice lacking the Tmprss2-encoded protease.* Mol Cell Biol, 2006. **26**(3): p. 965-75.
17. Kuba, K., et al., *A crucial role of angiotensin converting enzyme 2 (ACE2) in SARS coronavirus-induced lung injury.* Nat Med, 2005. **11**(8): p. 875-9.
18. Iwata-Yoshikawa, N., et al., *TMPRSS2 Contributes to Virus Spread and Immunopathology in the Airways of Murine Models after Coronavirus Infection.* J Virol, 2019. **93**(6).
19. Lin, B., et al., *Prostate-localized and androgen-regulated expression of the membrane-bound serine protease TMPRSS2.* Cancer Res, 1999. **59**(17): p. 4180-4.
20. Clinckemalie, L., et al., *Androgen regulation of the TMPRSS2 gene and the effect of a SNP in an androgen response element.* Mol Endocrinol, 2013. **27**(12): p. 2028-40.
21. Cano, L.Q., et al., *The co-chaperone p23 promotes prostate cancer motility and metastasis.* Molecular Oncology, 2015. **9**(1): p. 295-308.
22. Brooke, G.N. and C.L. Bevan, *The role of androgen receptor mutations in prostate cancer progression.* Curr Genomics, 2009. **10**(1): p. 18-25.
23. Crawford, E.D., et al., *Androgen-targeted therapy in men with prostate cancer: evolving practice and future considerations.* Prostate Cancer Prostatic Dis, 2019. **22**(1): p. 24-38.
24. Nuhn, P., et al., *Update on Systemic Prostate Cancer Therapies: Management of Metastatic Castration-resistant Prostate Cancer in the Era of Precision Oncology.* Eur Urol, 2019. **75**(1): p. 88-99.
25. Wilson, C.M. and M.J. McPhaul, *A and B forms of the androgen receptor are expressed in a variety of human tissues.* Mol Cell Endocrinol, 1996. **120**(1): p. 51-7.
26. Mikkonen, L., et al., *Androgen receptor and androgen-dependent gene expression in lung.* Mol Cell Endocrinol, 2010. **317**(1-2): p. 14-24.

27. Dart, D.A., et al., *Visualising androgen receptor activity in male and female mice.* PLoS One, 2013. **8**(8): p. e71694.
28. Yoon, G., et al., *Direct activation of TGF-beta1 transcription by androgen and androgen receptor complex in Huh7 human hepatoma cells and its tumor in nude mice.* J Cell Biochem, 2006. **97**(2): p. 393-411.
29. Lin, P., et al., *Reduction of androgen receptor expression by benzo[alpha]pyrene and 7,8-dihydro-9,10-epoxy-7,8,9,10-tetrahydrobenzo[alpha]pyrene in human lung cells.* Biochem Pharmacol, 2004. **67**(8): p. 1523-30.
30. Jeong, Y., et al., *Research resource: Diagnostic and therapeutic potential of nuclear receptor expression in lung cancer.* Mol Endocrinol, 2012. **26**(8): p. 1443-54.
31. McCoy, J., et al., *Racial Variations in COVID-19 Deaths May Be Due to Androgen Receptor Genetic Variants Associated with Prostate Cancer and Androgenetic Alopecia. Are Anti-Androgens a Potential Treatment for COVID-19?* J Cosmet Dermatol, 2020.
32. Stopsack, K.H., et al., *TMPRSS2 and COVID-19: Serendipity or Opportunity for Intervention?* Cancer Discov, 2020. **10**(6): p. 779-782.
33. Montopoli, M., et al., *Androgen-deprivation therapies for prostate cancer and risk of infection by SARS-CoV-2: a population-based study (n=4532).* Ann Oncol, 2020.
34. Brooke, G.N., et al., *Engineered repressors are potent inhibitors of androgen receptor activity.* Oncotarget, 2014. **5**(4): p. 959-69.
35. Brooke, G.N., et al., *FUS/TLS is a novel mediator of androgen-dependent cell-cycle progression and prostate cancer growth.* Cancer Res, 2011. **71**(3): p. 914-24.
36. Dart, D.A., et al., *Novel Trifluoromethylated Enobosarm Analogues with Potent Antiandrogenic Activity In Vitro and Tissue Selectivity In Vivo.* Mol Cancer Ther, 2018. **17**(9): p. 1846-1858.
37. Gamazon, E.R., et al., *Using an atlas of gene regulation across 44 human tissues to inform complex disease- and trait-associated variation.* Nat Genet, 2018. **50**(7): p. 956-967.
38. Lukassen, S., et al., *SARS-CoV-2 receptor ACE2 and TMPRSS2 are primarily expressed in bronchial transient secretory cells.* EMBO J, 2020. **39**(10): p. e105114.
39. Need, E.F., et al., *The unique transcriptional response produced by concurrent estrogen and progesterone treatment in breast cancer cells results in upregulation of growth factor pathways and switching from a Luminal A to a Basal-like subtype.* BMC Cancer, 2015. **15**: p. 791.
40. Pihlajamaa, P., et al., *The phytoestrogen genistein is a tissue-specific androgen receptor modulator.* Endocrinology, 2011. **152**(11): p. 4395-405.
41. Fornes, O., et al., *JASPAR 2020: update of the open-access database of transcription factor binding profiles.* Nucleic Acids Res, 2020. **48**(D1): p. D87-D92.
42. Grant, C.E., T.L. Bailey, and W.S. Noble, *FIMO: scanning for occurrences of a given motif.* Bioinformatics, 2011. **27**(7): p. 1017-8.
43. Stelloo, S., et al., *Endogenous androgen receptor proteomic profiling reveals genomic subcomplex involved in prostate tumorigenesis.* Oncogene, 2018. **37**(3): p. 313-322.
44. Taberlay, P.C., et al., *Three-dimensional disorganization of the cancer genome occurs coincident with long-range genetic and epigenetic alterations.* Genome Res, 2016. **26**(6): p. 719-31.
45. Sahu, B., et al., *FoxA1 specifies unique androgen and glucocorticoid receptor binding events in prostate cancer cells.* Cancer Res, 2013. **73**(5): p. 1570-80.

46. Consortium, E.P., *An integrated encyclopedia of DNA elements in the human genome.* Nature, 2012. **489**(7414): p. 57-74.
47. Gertz, J., et al., *Distinct properties of cell-type-specific and shared transcription factor binding sites.* Mol Cell, 2013. **52**(1): p. 25-36.
48. Severson, T.M., et al., *Characterizing steroid hormone receptor chromatin binding landscapes in male and female breast cancer.* Nat Commun, 2018. **9**(1): p. 482.
49. Zarnegar, M.A., et al., *Targeted chromatin ligation, a robust epigenetic profiling technique for small cell numbers.* Nucleic Acids Res, 2017. **45**(17): p. e153.
50. Glont, S.E., I. Chernukhin, and J.S. Carroll, *Comprehensive Genomic Analysis Reveals that the Pioneering Function of FOXA1 Is Independent of Hormonal Signaling.* Cell Rep, 2019. **26**(10): p. 2558-2565 e3.
51. He, H., et al., *c-Jun/AP-1 overexpression reprograms ERalpha signaling related to tamoxifen response in ERalpha-positive breast cancer.* Oncogene, 2018. **37**(19): p. 2586-2600.
52. Consortium, G.T., et al., *Genetic effects on gene expression across human tissues.* Nature, 2017. **550**(7675): p. 204-213.
53. Rockx, B., et al., *Comparative pathogenesis of COVID-19, MERS, and SARS in a nonhuman primate model.* Science, 2020. **368**(6494): p. 1012-1015.
54. Torjesen, P.A. and L. Sandnes, *Serum testosterone in women as measured by an automated immunoassay and a RIA.* Clin Chem, 2004. **50**(3): p. 678.
55. Sedelaar, J.P. and J.T. Isaacs, *Tissue culture media supplemented with 10% fetal calf serum contains a castrate level of testosterone.* Prostate, 2009. **69**(16): p. 1724-9.
56. Hay, C.W., et al., *Negative regulation of the androgen receptor gene through a primate-specific androgen response element present in the 5' UTR.* Horm Cancer, 2014. **5**(5): p. 299-311.
57. Leach, D.A., et al., *Cell-lineage specificity and role of AP-1 in the prostate fibroblast androgen receptor cistrome.* Mol Cell Endocrinol, 2017. **439**: p. 261-272.
58. Mangelsdorf, D.J., et al., *The nuclear receptor superfamily: the second decade.* Cell, 1995. **83**(6): p. 835-9.
59. Student, S., et al., *Anti-androgen hormonal therapy for cancer and other diseases.* Eur J Pharmacol, 2020. **866**: p. 172783.
60. Rice, M.A., S.V. Malhotra, and T. Stoyanova, *Second-Generation Antiandrogens: From Discovery to Standard of Care in Castration Resistant Prostate Cancer.* Front Oncol, 2019. **9**: p. 801.
61. Mina, A., R. Yoder, and P. Sharma, *Targeting the androgen receptor in triple-negative breast cancer: current perspectives.* Onco Targets Ther, 2017. **10**: p. 4675-4685.

FIGURE LEGENDS

Figure 1. TMPRSS2 is an androgen regulated gene in LNCaP cells. A) LNCaP were incubated in hormone-depleted media for 72 hrs and treated ± 1 nM mibolerone (MIB) ± 10 μM enzalutamide (ENZ) for 24 hrs. RNA was harvested, reverse transcribed and qPCR performed to quantify the expression of *TMPRSS2*. Mean of 3 independent repeats (± 1SEM). ANOVA, * p<0.05 MIB vs VC (vehicle control), #p<0.05 MIB + ENZ. Data from B) MCF-7 cells (GSE99626, N=2) and C) T47D cells (GSE662243, N=3) treated with 10nM DHT were analysed for TMPRRS2 expression. Significance determined using ANOVA, * p<0.05.

Figure 2. TMPRSS2 and the AR are expressed in the lung. A) The GTEx dataset [52] was interrogated and median expression of AR was plotted against median TMPRSS2 expression. Data is expressed as each gene normalised across all tissues (z-score). **B)** Single-cell analysis of lung tissue [38] was interrogated and cells expressing titled gene are marked in black, negative cells are in light blue. **C)** Breakdown of AR, TMPRSS2, and ACE2 expression levels in specific lung cell types (X-axis); Y Axis denotes gene mRNA CPM.

Figure 3. TMPRSS2 is expressed at higher levels in the male lung compared to female lung. The GTEx dataset [52] was interrogated and expression of AR and TMPRSS2 investigated in lung tissue and dichotomized by gender, M = male (N=220), F = female (N=355). Significance tested via Wilcoxin, * P<0.05. Circles denote statistical outliers (2 x inter quartile range).

Figure 4. AR is expressed in the A549 lung cell line. A) A549 and LNCaP cells were lysed and proteins separated using SDS-PAGE. Immunoblotting was performed to visualise AR expression levels and α-tubulin was used as a loading control. **B)** LNCaP and A549 were incubated in full media for 48 hrs or 72 hours + 10 nM mibolerone ± 10 μM enzalutamide. RNA was harvested, reverse transcribed and qPCR performed to quantify the expression of *TMPRSS2*. Mean of 3 independent repeats (± 1SEM). ANOVA, *** p<0.0005.

Figure 5. Enzalutamide successfully down-regulates TMPRSS2 in mouse lung. A) Relative expression of *Ar*, *Tmprss2*, and *Ace2* mRNA from lung tissue of mice treated with enzalutamide (n=9) or vehicle control (VC, n=8) once daily for 3 days. Expression was normalised to housekeeping genes and made relative to VC. **B)** Log2 expression of *Tmprss2*, *Ar*, and *Ace2* in lung tissue from male mice physically castrated (N=3) vs intact male mice (N=3) (GSE31341). Statistical analysis was performed using Student T test, * p< 0.05, ** p<0.01, *** p<0.001.

Figure 6. Potential regulatory regions in the TMPRSS2 promoter. ChIP sequencing peaks of AR, FOXA1, GR, and H3K27ac in LNCaP cells, FOXA1, JUN, GR, and H3K27ac in A549 lung cells, AR, H3K27ac, FOXA1, JUN, GR, ESR1 in MCF-7 breast cancer cells. The TMPRSS2 gene is highlighted in the purple shaded box and the potential regulatory region 1 is boxed in yellow, the potential regulatory region 2 is boxed in orange. Potential AREs are marked in blue boxes (MA0007.2) or green (determined by [20]) **B)** AR motif MA0007.2 from JASPAR curated motif database. **C)** Position of potential MA0007.2 motifs around the TMPRSS2 gene separated into two regions, the first region (regulatory region 1 covering areas of TSS and promoter/enhancers, the second region (regulatory region 2) covers more distant enhancer regions.

Figure 7. Schematic representation of how targeting the AR could reduce SARS-CoV-2 entry.

Leach et al. Figure 1

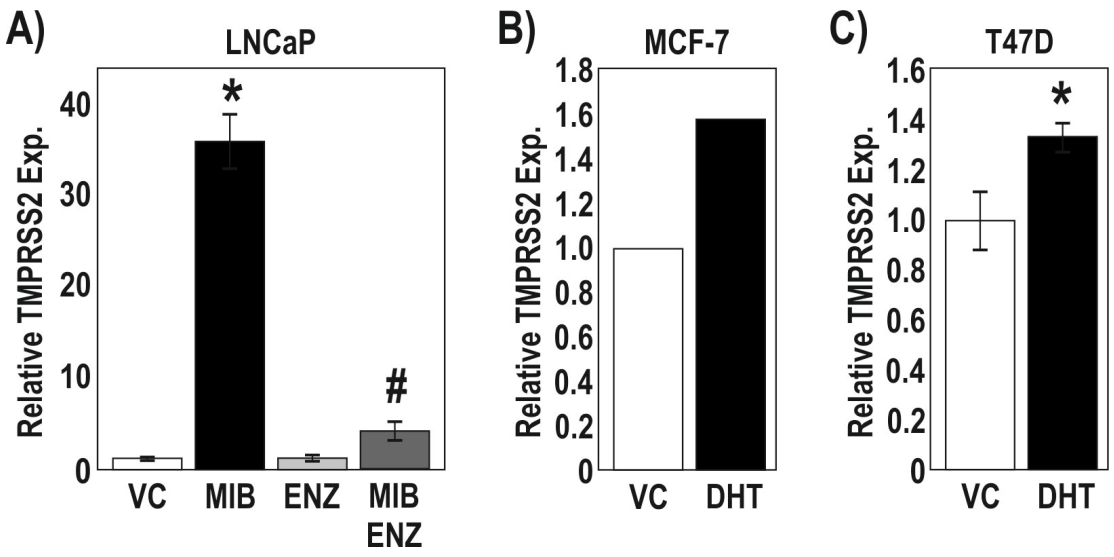

Leach et al. Figure 2

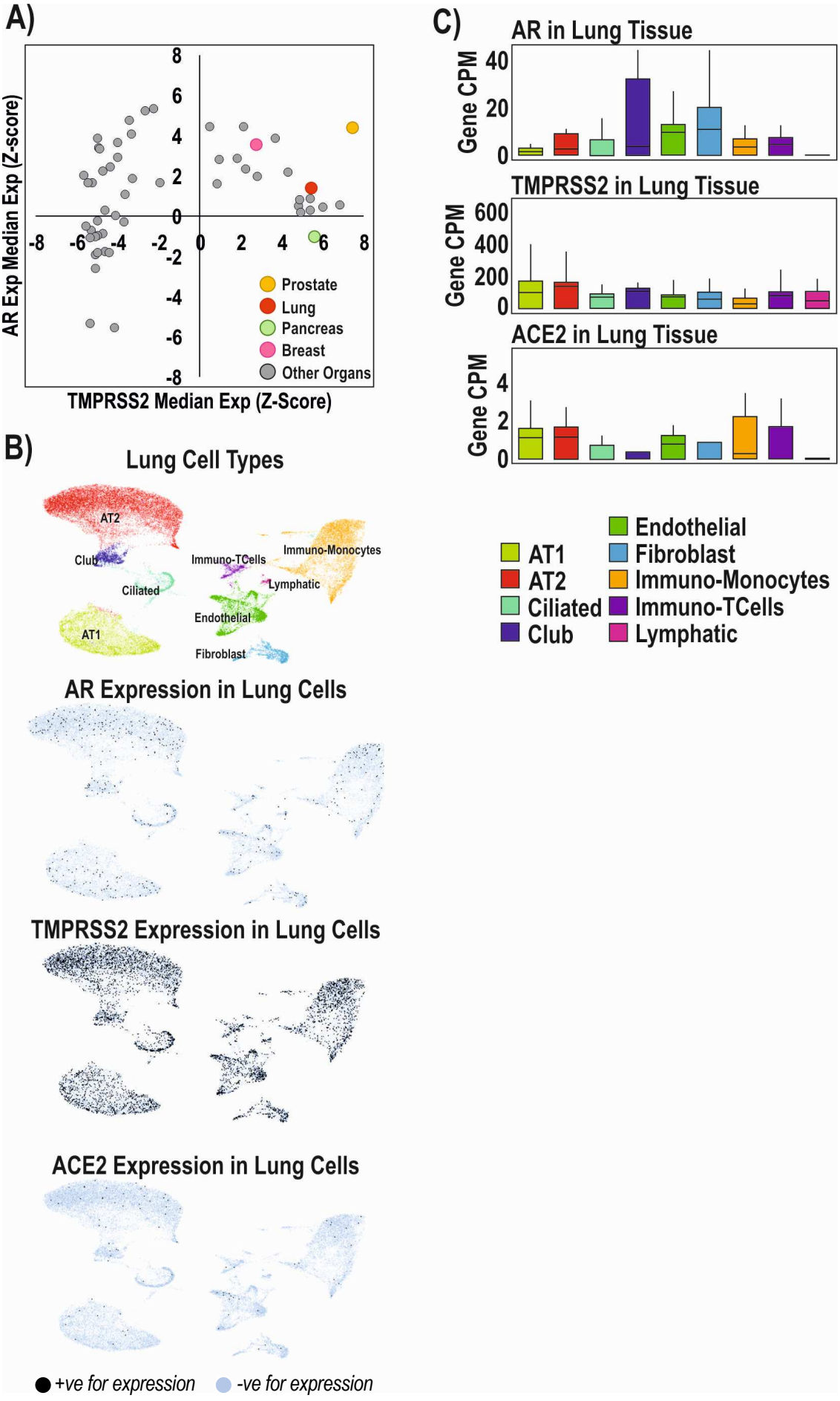

Leach et al. Figure 3

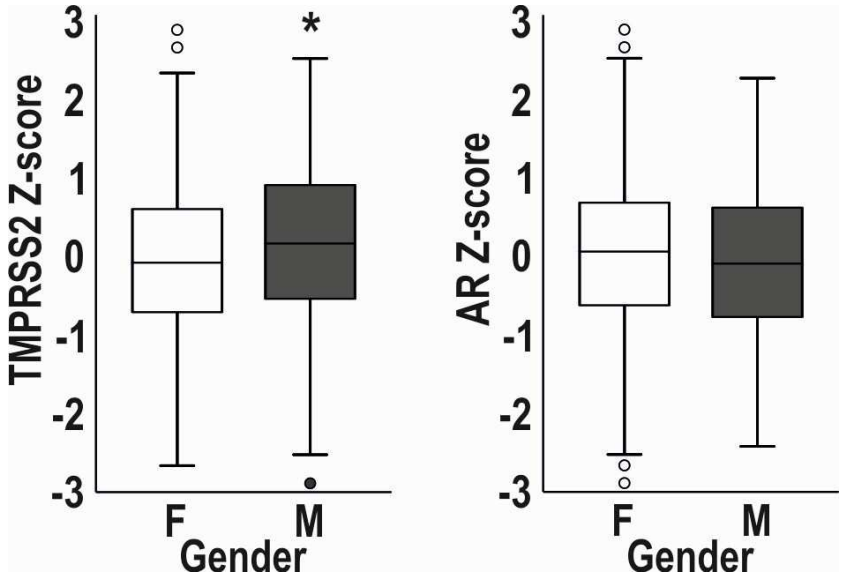

Leach et al. Figure 4

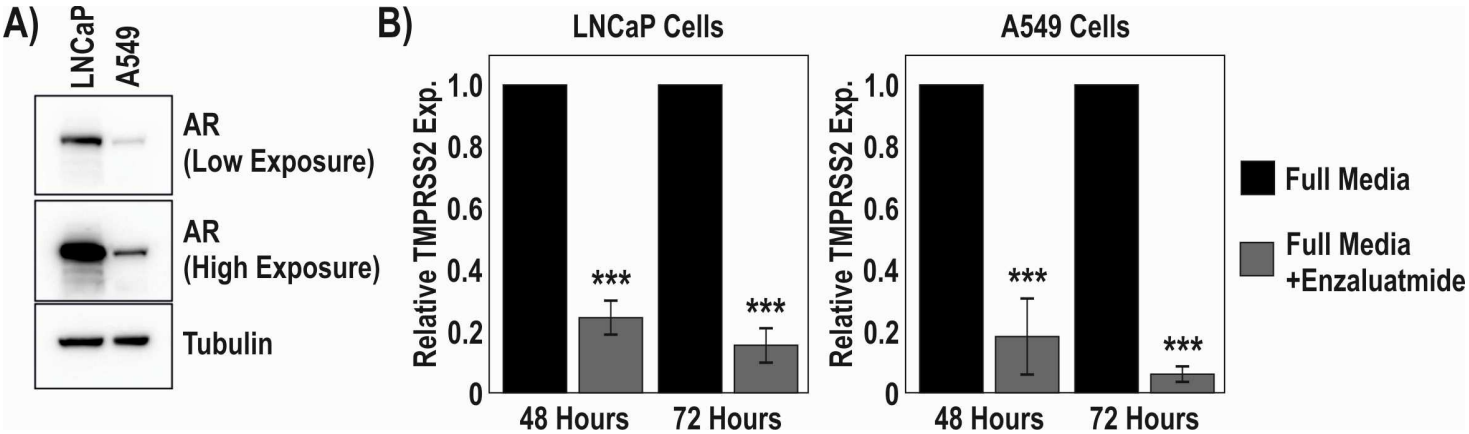

Leach et al. Figure 5

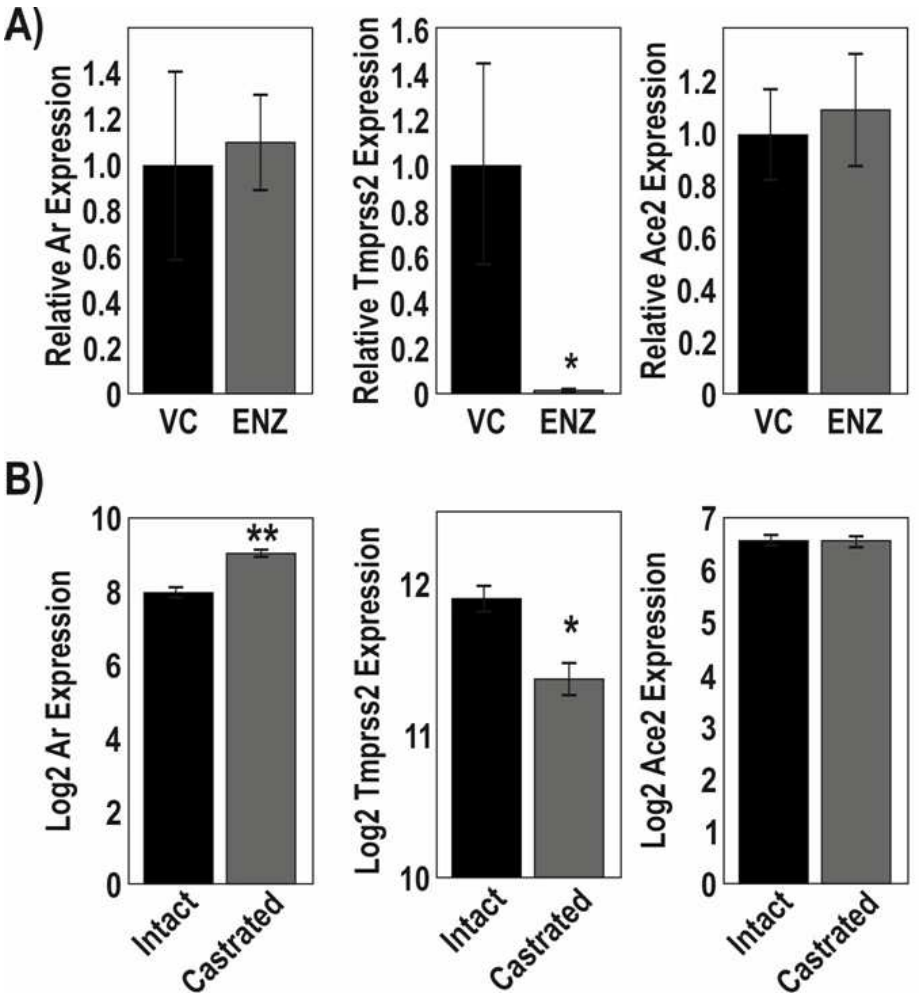

Leach et al. Figure 6

A)

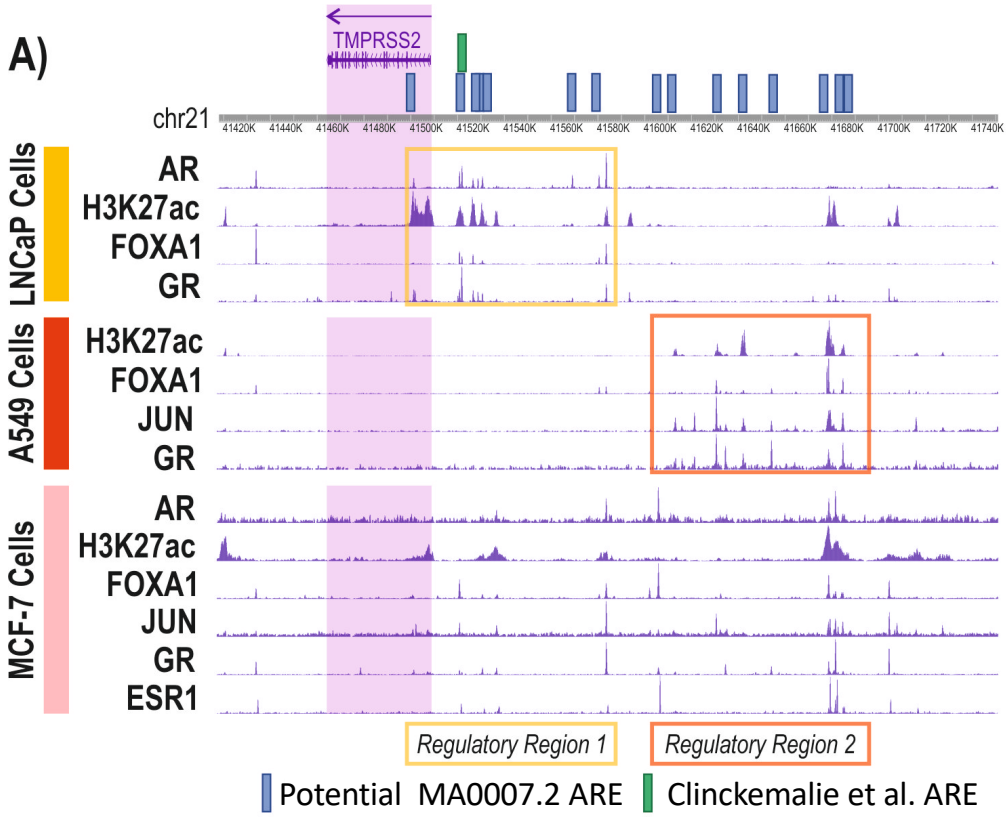

B)

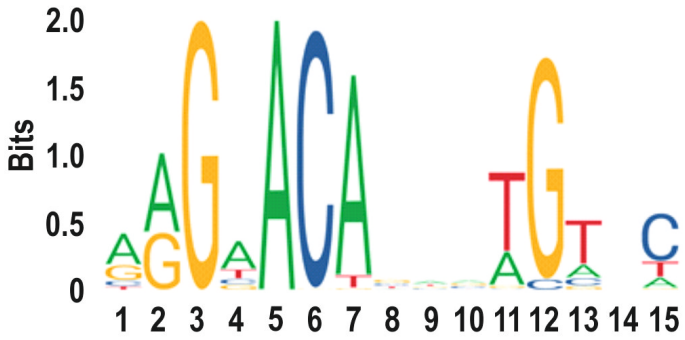

C)

Regulatory region 1 Chr21:41490000-41580500

		Start	End	Strand	p-value	Matched Sequence
MA0007.2	Chr21	41498078	41498092	-	0.0000367	AAGAACTGTAAGTAC
MA0007.2	Chr21	41521454	41521468	+	0.0000198	GGGCACAGCCTGAGC
MA0007.2	Chr21	41521553	41521567	-	0.0000737	CAGAACAGCCTGTGG
MA0007.2	Chr21	41528878	41528892	-	0.0000652	CAGAACATTATGGAC
MA0007.2	Chr21	41529170	41529184	-	0.0000354	GGGCACACGCTGTTA
MA0007.2	Chr21	41532582	41532596	+	0.0000215	GAGAACAGTGGGTTC
MA0007.2	Chr21	41569350	41569364	-	0.000068	AGGAACACCGGGAGC
MA0007.2	Chr21	41578975	41578989	+	9.64E-07	GAGAACATCGTGTGC

Regulatory region 2 Chr21:4160000-41690500

		Start	End	Strand	p-value	Matched Sequence
MA0007.2	Chr21	41605770	41605784	-	0.0000931	AGGTACAAAATGAAA
MA0007.2	Chr21	41611959	41611973	-	0.0000994	AGGTACACACTGATG
MA0007.2	Chr21	41630148	41630162	-	0.00000491	AAGTACAGAGTGCGC
MA0007.2	Chr21	41642129	41642143	-	0.0000122	GGGAACAGGCAGTGT
MA0007.2	Chr21	41656029	41656043	-	0.0000922	AGGTACAAAGGGTAC
MA0007.2	Chr21	41676130	41676144	+	0.000068	AAGAACACTGTGAGG
MA0007.2	Chr21	41683746	41683760	+	0.0000209	GGGAACAGAAAGGGC
MA0007.2	Chr21	41687334	41687348	+	0.0000314	CAGCACAGAGTGAAC

Leach et al. Figure 7

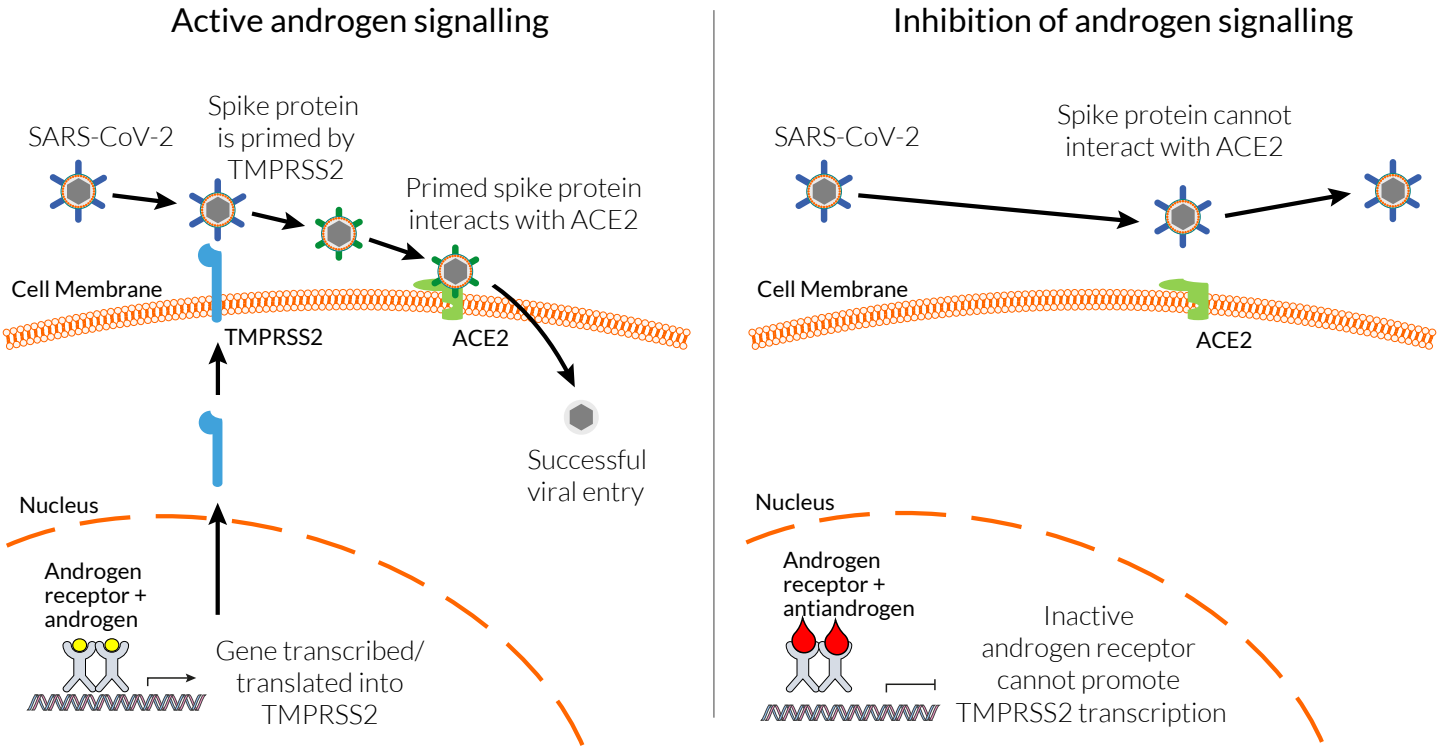

Figures

Leach et al. Figure 1

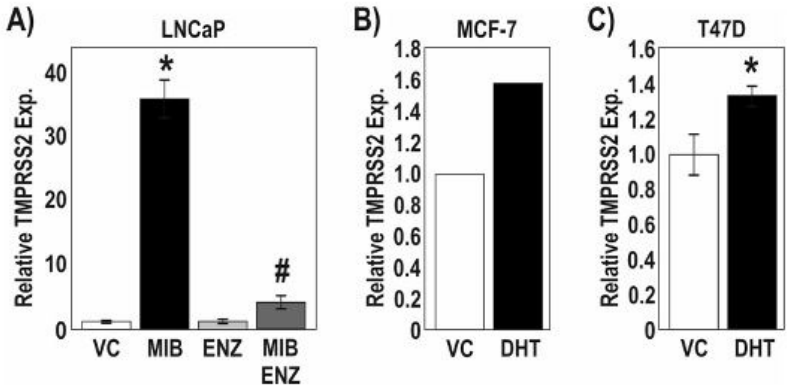

Figure 1

TMPRSS2 is an androgen regulated gene in LNCaP cells. A) LNCaP were incubated in hormone- depleted media for 72 hrs and treated ± 1 nM mibolerone (MIB) ± 10 μM enzalutamide (ENZ) for 24 hrs. RNA was harvested, reverse transcribed and qPCR performed to quantify the expression of TMPRSS2. Mean of 3

independent repeats (± 1SEM). ANOVA, * p<0.05 MIB vs VC (vehicle control), #p<0.05 MIB + ENZ. Data from B) MCF-7 cells (GSE99626, N=2) and C) T47D cells (GSE662243, N=3) treated with 10nM DHT were analysed for TMPRRS2 expression. Significance determined using ANOVA, * p<0.05.

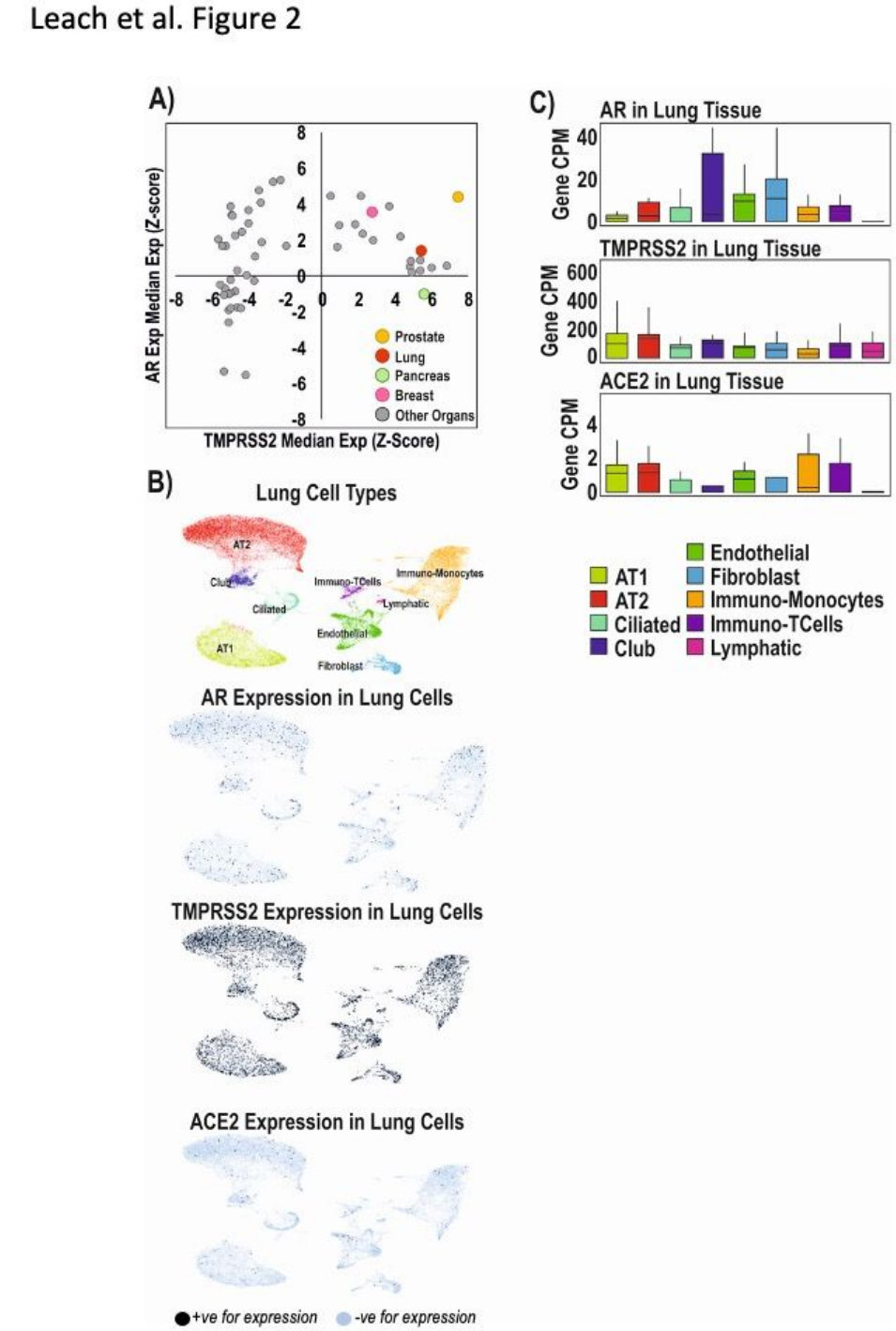

Figure 2

TMPRSS2 and the AR are expressed in the lung. A) The GTEx dataset [52] was interrogated and median expression of AR was plotted against median TMPRSS2 expression. Data is expressed as each gene

normalised across all tissues (z-score). B) Single-cell analysis of lung tissue [38] was interrogated and cells expressing titled gene are marked in black, negative cells are in light blue. C) Breakdown of AR, TMPRSS2, and ACE2 expression levels in specific lung cell types (X-axis); Y Axis denotes gene mRNA CPM.

Leach et al. Figure 3

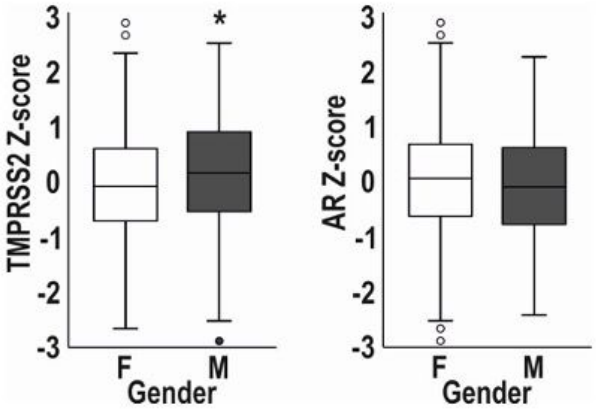

Figure 3

TMPRSS2 is expressed at higher levels in the male lung compared to female lung. The GTEx dataset [52] was interrogated and expression of AR and TMPRSS2 investigated in lung tissue and dichotomized by gender, M = male (N=220), F = female (N=355). Significance tested via Wilcoxin, * P<0.05. Circles denote statistical outliers (2 x inter quartile range).

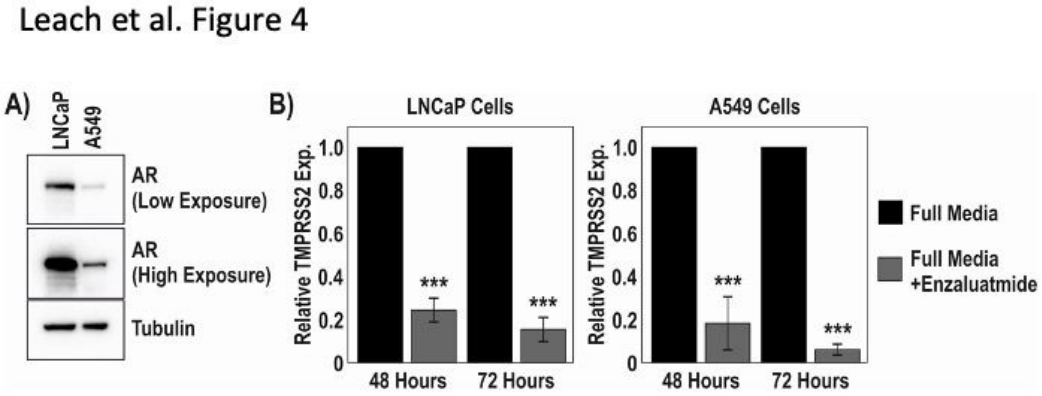

Figure 4

AR is expressed in the A549 lung cell line. A) A549 and LNCaP cells were lysed and proteins separated using SDS-PAGE. Immunoblotting was performed to visualise AR expression levels and a-tubulin was used as a loading control. B) LNCaP and A549 were incubated in full media for 48 hrs or 72 hours + 10 nM mibolerone ± 10 μM enzalutamide. RNA was harvested, reverse transcribed and qPCR performed to quantify the expression of TMPRSS2. Mean of 3 independent repeats (± 1SEM). ANOVA, *** p<0.0005.

Leach et al. Figure 5

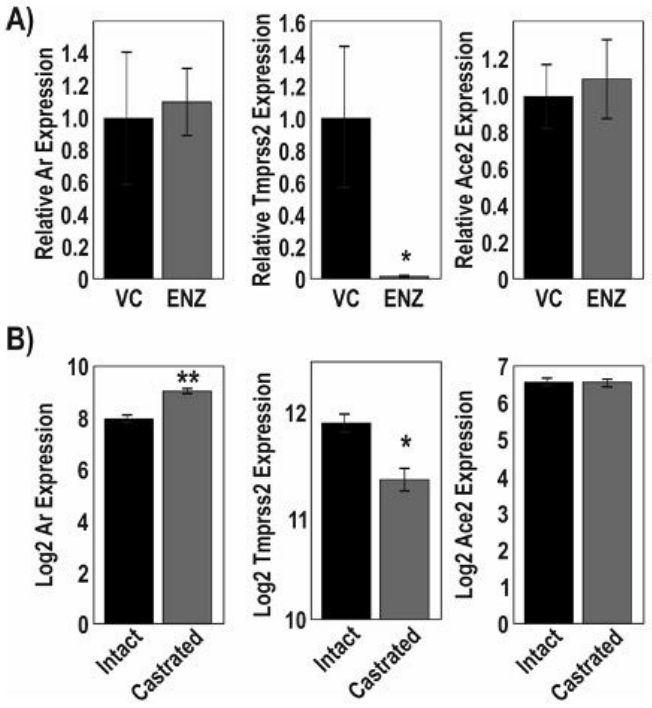

Figure 5

Enzalutamide successfully down-regulates TMPRSS2 in mouse lung. A) Relative expression of Ar, Tmprss2, and Ace2 mRNA from lung tissue of mice treated with enzalutamide (n=9) or vehicle control (VC, n=8) once daily for 3 days. Expression was normalised to housekeeping genes and made relative to VC. B) Log2 expression of Tmprss2, Ar, and Ace2 in lung tissue from male mice physically castrated (N=3) vs intact male mice (N=3) (GSE31341). Statistical analysis was performed using Student T test, * p< 0.05, ** p<0.01, *** p<0.001.

Leach et al. Figure 6

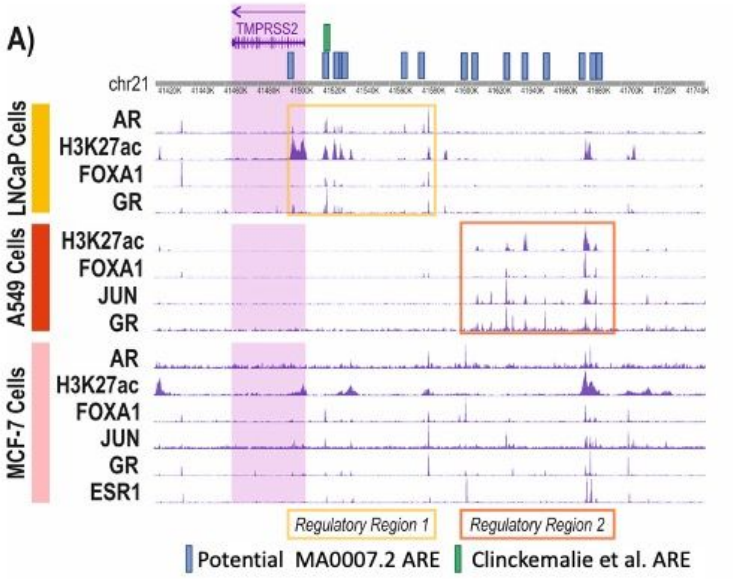

C)

Regulatory region 1 Chr21:41490000-41580500

		Start	End	Strand	p-value	Matched Sequence
MA0007.2	Chr21	41498078	41498092	-	0.0000367	AAGAACTGTAAGTAC
MA0007.2	Chr21	41521454	41521468	+	0.0000198	GGGCACAGCCTGAGC
MA0007.2	Chr21	41521553	41521567	-	0.0000737	CAGAACAGCCTGTGG
MA0007.2	Chr21	41528878	41528892	-	0.0000652	CAGAACATTATGGAC
MA0007.2	Chr21	41529170	41529184	-	0.0000354	GGGCACACGCTGTTA
MA0007.2	Chr21	41532582	41532596	+	0.0000215	GAGAACAGTGGGTTC
MA0007.2	Chr21	41569350	41569364	-	0.000068	AGGAACACCGGGAGC
MA0007.2	Chr21	41578975	41578989	+	9.64E-07	GAGAACATCGTGTGC

Regulatory region 2 Chr21:4160000-41690500

		Start	End	Strand	p-value	Matched Sequence
MA0007.2	Chr21	41605770	41605784	-	0.0000931	AGGTACAAAATGAAA
MA0007.2	Chr21	41611959	41611973	-	0.0000994	AGGTACACACTGATG
MA0007.2	Chr21	41630148	41630162	-	0.00000491	AAGTACAGAGTGCGC
MA0007.2	Chr21	41642129	41642143	-	0.0000122	GGGAACAGGCAGTGT
MA0007.2	Chr21	41656029	41656043	-	0.0000922	AGGTACAAAGGGTAC
MA0007.2	Chr21	41676130	41676144	+	0.000068	AAGAACACTGTGAGG
MA0007.2	Chr21	41683746	41683760	+	0.0000209	GGGAACAGAAAGGGC
MA0007.2	Chr21	41687334	41687348	+	0.0000314	CAGCACAGAGTGAAC

Figure 6

Potential regulatory regions in the TMPRSS2 promoter. ChIP sequencing peaks of AR, FOXA1, GR, and H3K27ac in LNCaP cells, FOXA1, JUN, GR, and H3K27ac in A549 lung cells, AR, H3K27ac, FOXA1, JUN, GR, ESR1 in MCF-7 breast cancer cells. The TMPRSS2 gene is highlighted in the purple shaded box and the potential regulatory region 1 is boxed in yellow, the potential regulatory region 2 is boxed in orange. Potential AREs are marked in blue boxes (MA0007.2) or green (determined by [20]) B) AR motif MA0007.2 from JASPAR curated motif database. C) Position of potential MA0007.2 motifs around the TMPRSS2 gene separated into two regions, the first region (regulatory region 1 covering areas of TSS and promoter/enhancers, the second region (regulatory region 2) covers more distant enhancer regions.

Leach et al. Figure 7

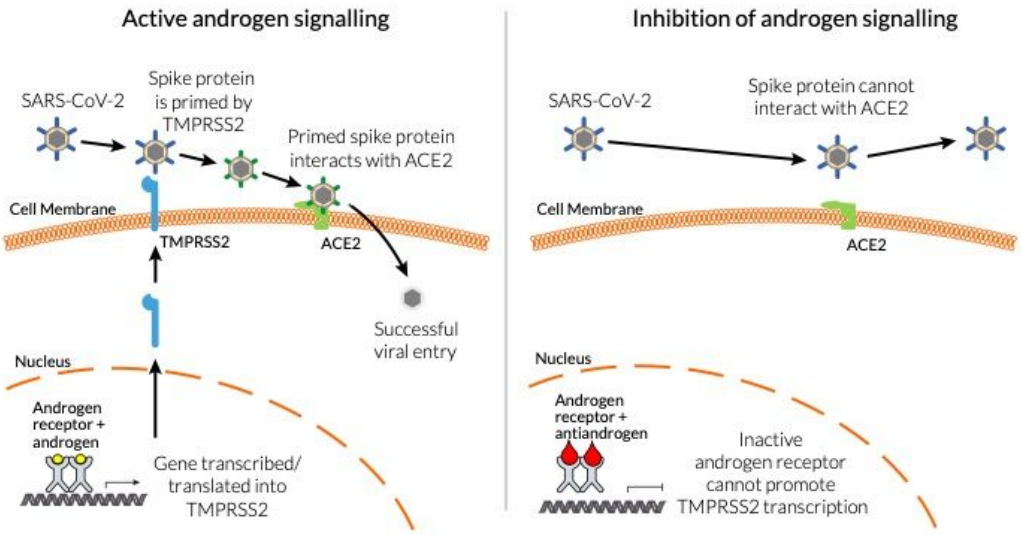

Figure 7

Schematic representation of how targeting the AR could reduce SARS-CoV-2 entry.